International Journal of Engineering Inventions
e-ISSN: 2278-7461, p-ISSN: 2319-6491
Volume 13, Issue 5 [May. 2024] PP: 06-14

Finite element analysis of spine biomechanics based on ANSYS

HE Chunshan，DOU Shixin，MA Xiaoying, HOU Zhenhua
Institute of Mechanical and Vehicle Engineering,Changchun University
Corresponding Author: HOU Zhenhua

ABSTRACT: *A finite element model of the spine was established to observe the effects of different moment loads on the stability of the human spine and the kinetic properties of the spine, in order to avoid scoliosis and ensure the healthy growth of the spine. Through the CT scan data, the 3D image of the spine was extracted in Mimics software, and the bone inverse processing was carried out using Geomagic Studio software, and the 3D model of the T_7-T_{11} segments was established by graphic optimisation one by one, and the finite element simulation was carried out in ANSYS software. A torsional load of 10 N•m was applied, and 8.6° of forward flexion, 4.5° of backward extension, 8.8° of left lateral bending, and 9.1° of right lateral bending were measured; the results obtained were similar to those of literatures., et al. The validity of the finite element model was verified. Three different moments of 10 N•m, 30 N•m and 50 N•m were applied, and the maximum displacement of the spine was measured to be 1.3033 mm, 3.4275 mm and 5.6641 mm, respectively. By extracting the first 6 orders of free modes of the spine, the dynamic characteristics of the spine segments T_7-T_{11} are obtained, and the segments T_7-T_9 are the most severely deformed segments of the spine model, which are more prone to larger deformations than the other segments. After finite element analysis, it is known that when the moment load is taken as 30 N•m, the critical value of the spine displacement value is reached and the spine is in a stable state. When the moment load reaches 50 N•m, the spine is in an unstable state. According to the dynamic characteristics of the spine, the modal intrinsic frequency of the spine is mainly concentrated in the range of 6-35Hz, and the human body should be prevented from entering this frequency range to avoid damage to the spine.*

Keywords: *Finite element analysis;Modal analysis;Moment load;Maximum displacement*

Date of Submission: 24-04-2024 Date of acceptance: 02-05-2024

I. INTRODUCTION

The current social situation and work patterns have changed considerably, and people's health awareness is gradually increasing, with more and more people becoming aware of the health hazards of disease, If scoliosis is not treated quickly and effectively, the spinal deformity can progress rapidly and lead to various complications [1].Biomechanical analysis of the spine is an important method for the diagnosis and treatment of scoliosis [2].

Finite Element Analysis (FEA) is a mechanical analysis technique that discretises into a finite number of small units, applies material properties, and makes physical connections to obtain an overall calculus equation through which biomechanical calculations and analyses can be performed [3].The finite element modelling methods currently used in spinal biomechanics research mainly use equipment such as thin-layer CT and high-resolution MRI to obtain three-dimensional coordinate data of the vertebral body and its affiliated tissue structures, and to derive the stress, position, morphology, and mesenchymal changes between each part according to the movement of the human spine and the relative motion between the vertebrae in order to investigate their biomechanical changes [4]. Gao Mingjie et al [5] analysed the biomechanical changes of the lumbar spine after lumbar foramenoplasty of different degrees of lumbar spine, and in adolescent lumbar foramenoplasty, the clinic should be cautious in removing more than 1/2 or more of the articular surface of the articular eminence to avoid lumbar spine instability. Hurwitz et al [6] summarised findings from the Global Burden of Disease (GBD) report in relation to low back and neck pain, with prevalence and disability increasing significantly with low back and neck pain and likely to rise further as the population ages. Brittany et al [7] developed two finite element models of the spine through finite element modelling, through which it was found that females are more likely to suffer from spinal disorders compared to males. Alex K. et al [8] validated a parametric finite element model of the thoracolumbar spine, including its ability to predict the biomechanical effects of varying the amount of EOS-corrected polyethylene sublaminar tape levels detected in growth-guided structures. Ni et al [9] simulated 32 different scoliosis curves using a flexible spine model, with each curvature

imaged accordingly using DR, CR and EOS systems. Zhu et al [10] used Abaqus to establish a three-dimensional finite element model of the lumbosacral spine, which effectively accomplished the construction of the spine model and made up for the defects of the single motion segment model. Li Rui et al [11] established a three-dimensional finite element model from imaging data of patients with atlantoaxial disorders, analysed the stresses on the articular surfaces and intervertebral discs, and demonstrated that atlantoaxial disorders can be detrimental to the upper cervical spine as a whole, which may lead to neck pain and spinal degeneration. Guo et al [12] studied the biomechanical properties of the spine and created a three-dimensional nonlinear finite element model of the human spine using finite element techniques. The model provides a more realistic theoretical framework for the study of spinal biomechanics in clinical medicine and ergonomics. M Xu et al [13] By performing biomechanical analysis of the spine, a combination of predictions from several different cell models can be obtained, which can be used to improve the prediction of the behaviour of the human lumbar spine under the same loads and boundary conditions.

II. Information and methodology

Three-dimensional modelling of the spine

In this paper, biomechanical analyses of the T_7-T_{11} segments of the human spine were performed to investigate their mechanical properties. The cross-sectional images of healthy human bone windows were obtained by CT scanning, in which different human tissues have different densities, corresponding to different grey values in the CT images [14], as shown in Table 1.

Table 1 CT thresholds for each site

Part name	Thresholds
Femoral	225HU-3071HU
Knee	226HU-1765HU
Columna vertebralis	150HU-1368HU
Hip joint	200HU-1681HU
Lumbar vertebra	226HU-1753HU

The CT images were imported into Mimics to extract the 3D image data of the spine and different bone separations were performed based on functions such as threshold segmentation and mask creation. The 3D image data was imported into Geomagic Studio and optimised graphically one by one, i.e., the model was subjected to a series of operations such as hole filling, smoothing, relaxation, deletion of pegs, noise reduction, etc. to obtain a model with no sharp corners and holes, and this obtained model was imported into ANSYS to perform the biomechanical finite element analysis, and meshing was performed; The flowchart of spine 3D model extraction is shown in Fig. 1, and finally the complete human spine 3D finite element model is established. The process flow chart is shown in Figure 2.

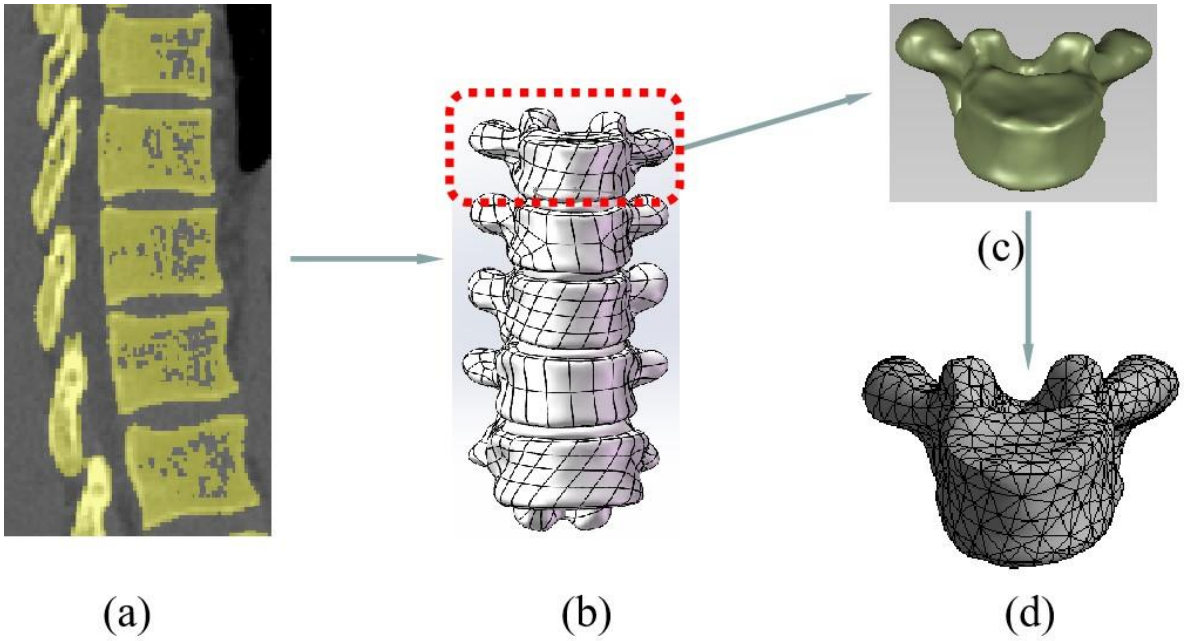

Fig. 1 Flowchart of spine 3D model extraction

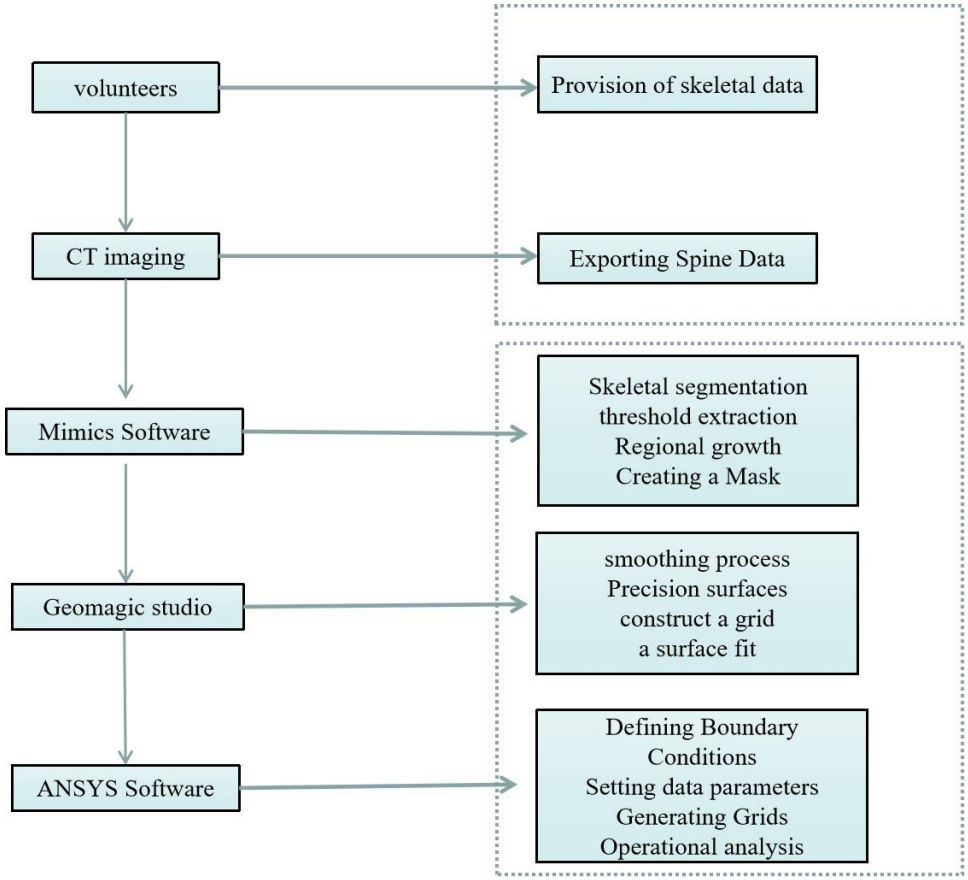

Fig. 2 CT extraction and finite element analysis

Material properties

In order to make the model more in line with the actual structure of the human body, the vertebrae are subdivided into periosteum, cortical bone, cancellous bone, etc. According to the modulus of elasticity and Poisson's ratio of the different bone materials, the values of the materials for the cortical bone, cancellous bone, articular cartilage, and other parts of the vertebrae are determined. Luo Huiqing et al [15] divided the vertebral

body and lumbar intervertebral disc into 1 mm thick cortical and cancellous bone, set the materials according to the homogeneity of each, and analysed the vertebral body stresses by modulus of elasticity and Poisson's ratio. Dai Yunlei et al [16] In order to analyse the stresses in the various parts of the spinal structure, the modulus of elasticity of the bone was taken as 12 Gpa and Poisson's ratio was taken as 0.3; a pressure load with a magnitude of 500 N vertically downward was applied on the upper surface of the vertebral body, while at the same time a torsional load of 10 $N \cdot m$ was applied at the nodes of this surface. Snapdragon Yang et al [17] applied 4 $N \cdot m$ torque in different directions on the upper surface of the thoracic vertebra T_1 and 10 $N \cdot m$ torque in different directions on the upper surface of the lumbar sacral T_1 segment, and calculated the ROM and the average stiffness of the vertebral body in anterior and posterior flexion and extension, left and right rotation, and left and right lateral flexion and extension, and in flexion and extension, rotation, and lateral flexion and extension. Kuo Tu-Sheng [18] analysed the stress field of the knee joint by assigning material properties to the knee joint model. The unit types and material properties of each component of the spine are shown in Table 2.

Table 2 Skeletal material parameters

Place	Modulus of elasticity（Mpa)	Poisson's ratio
Cortical bone	1200	0.300
Cancellous bone	100	0.200
Endplate	25	0.250
Nucleus Pulposus	1	0.499
Fibre ring	4.2	0.450
Gristle	50	0.300

Load settings and boundary conditions

static analysis

The T_7-T_{11} segments of the spine were selected, and a pressure load of size 500 N vertically downward was applied to the upper surface of vertebra T_7, while a torsional load of 10 $N \cdot m$ was applied to the nodes of this surface and the upper surface of the spinous process to simulate the forward flexion motion, the backward extension motion, the left lateral bending motion, and the right lateral bending motion, and to extract the results of stress distribution of each vertebra in this model. Ninety per cent of the load is applied to the anterior and middle columns and 15 per cent to the posterior column.The T_{11} vertebrae are fixed in any direction.

modal analysis

The classical definition of modal analysis is to transform the physical coordinates in a system of vibrational differential equations for a linear stationary system into modal coordinates, so that the system of equations is decoupled and becomes a set of independent equations described in terms of modal coordinates and modal parameters in order to find the modal parameters of the system.

Modal analysis is the basis of dynamic analysis, the most important factors in modal analysis are the properties of the structure itself and the properties of the material, modal analysis transforms the dynamic problems of complex elastomers into simple static problems. The modal parameters of the dynamic characteristics of the system are calculated from the following differential equation of motion (1).

$$[M]\{\ddot{x}\} + [C]\{\dot{X}\} + [K]\{x\} = \{F(t)\} \tag{1}$$

Where, $[M]$、$\{x\}$、$[C]$、$[K]$、$\{F(t)\}$ are the mass of the system, the displacement vectors at each point, the damping, the stiffness matrix and the excitation vectors at each point, respectively.

In the case of free vibration, neglecting damping, it follows that $[C] = 0, \{F(t)\} = 0$, giving Equation (2).

$$[M]\{\ddot{x}\} + [K]\{x\} = 0 \tag{2}$$

The free vibration of the elastomer produces a series of simple harmonic vibrations, i.e., $\{x(t)\} = \{\varphi\}\sin\{\omega t\}$ yielding the equation shown in (3).

$$([K] - \omega^2[M])\{\varphi\} = \{0\} \tag{3}$$

Assuming that the amplitude $\{\varphi\}$ is not all zero, this yields as shown in equation (4).

$$|-\omega^2[M] + [K]| = 0 \tag{4}$$

By solving the equation, there are n orders of intrinsic frequency $\{\omega_i\}$, i=1,2,3,...n, and then the corresponding amplitude value of each order of intrinsic frequency $\{\omega_i\}$ can be obtained by equation (3).

III. RESULTS

Validation of a finite element model of the thoracic segment of the spine (T_7-T_{11})

A pressure load of size 500 N vertically downward was applied to the upper surface of the T_7 vertebral body, while a torsional load of 10 $N•m$ was applied to the nodes of this surface, and the mobility of the T_7-T_9 segments was measured: anterior flexion of 8.6°, posterior extension of 4.5°, left lateral curvature of 8.8°, and right lateral curvature of 9.1°, and the results obtained were similar to the results of Ou, B.J. et al.[19], which proved the spine validity of the finite element model.

Finite element analysis of the model of thoracic vertebral segment of the spine (T_7-T_{11}) under different loads

A moment of 10 N•m, 30 N•m and 50 N•m was applied to the surface of T_7, while a pressure load of 700 N was applied to this surface to simulate the preloading of the weight of the human torso. According to the previous literature, it is known that the stability of the spine is judged by the magnitude of the displacement, so the displacement is also used as a reference criterion for this research object.

The maximum displacement of the spine was 1.3033 mm when a moment of 10 N•m, was applied to the upper surface of T_7, as shown in Fig. 3.

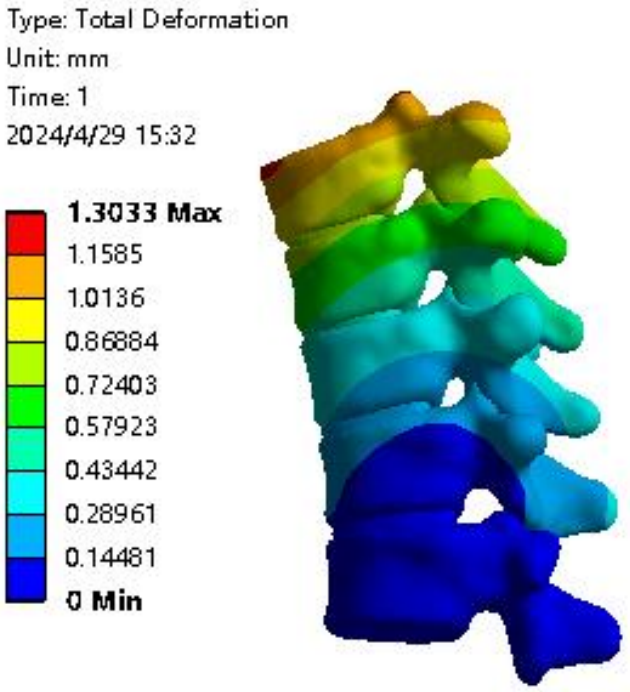

Fig. 3 Displacement diagram of 10 N•m FEA results

A moment of 30 N•m was applied to the upper surface of T_7, and the maximum displacement of its spine was 3.4275 mm, as shown in Fig. 4.

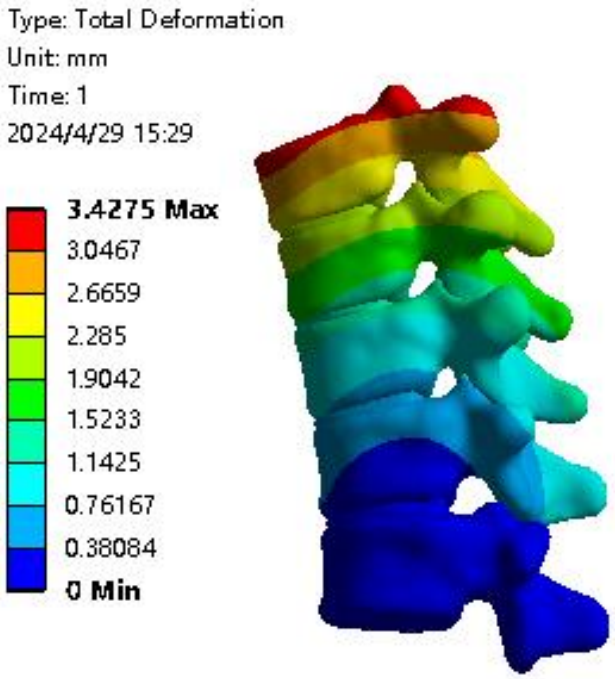

Fig. 4 Displacement diagram of 30 N•m FEA results

A moment of 50 N•m was applied to the upper surface of T_7, and the maximum displacement of its spine was 5.6641 mm, as shown in Fig. 5.

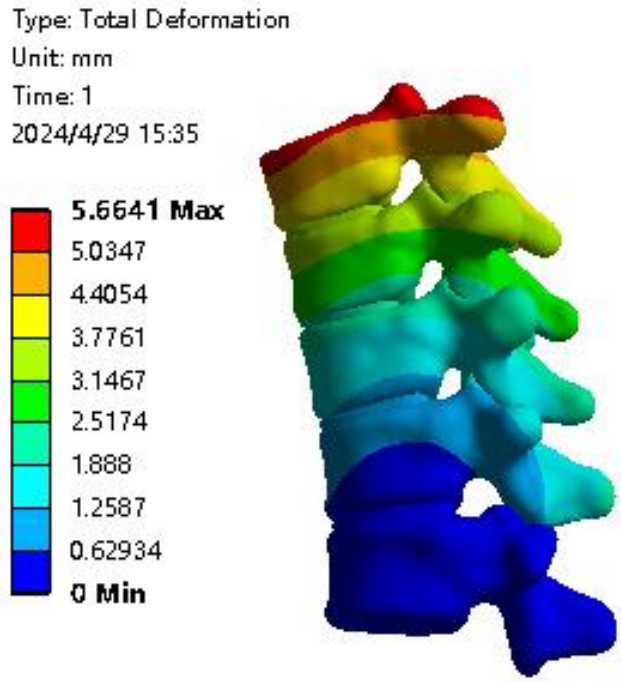

Fig. 5 Displacement diagram of 50 N•m FEA results

The above static analysis results show that: the maximum displacement in the thoracic spine T_7, T_8-T_9 thoracic spine displacement size followed, can be proved that the thoracic spine T_7-T_9 segments is the most likely to produce the maximum displacement of the site, the maximum displacement data are shown in Table 3; different moments under the T_7-T_{11} segments of the maximum displacement of the comparative chart in Fig. 6.

Table 3 Maximum displacement under different moments

Torques (N•m)	10	30	50
Maximum displacement(mm)	1.3033	3.4275	5.6641

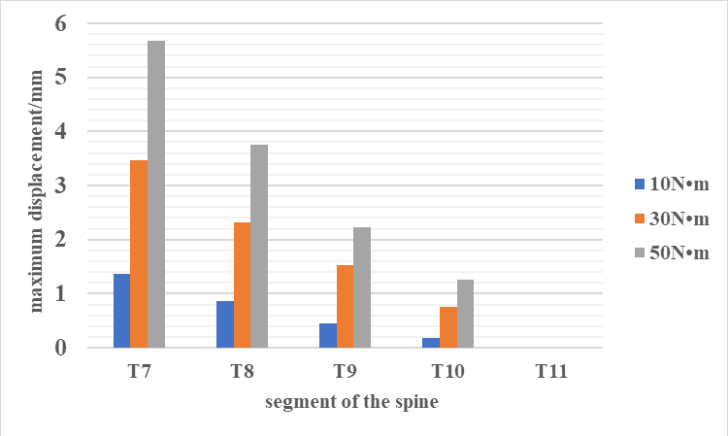

Fig 6 T_7-T_{11} section maximum displacement data map

According to domestic and foreign scholars research literature [20]-[21], the normal state of the spine activity displacement range of 3 mm-3.5 mm, when the activity displacement is less than 3 mm, the spine is in a stable state, when the activity displacement is greater than 3.5 mm, the spine is in an unstable state, which will increase the probability of suffering from spinal diseases.

Table 3 shows that when 10 N•m moment is applied, the maximum displacement is less than 3 mm; when 30 N•m moment is applied, the maximum displacement is more than 3 mm but less than 3.5 mm; when 50 N•m moment is applied, the maximum displacement is more than 3 mm, and the spine is in an unstable state; therefore, the human spine should not be loaded with more than 30 N•m moment for a long time, which will lead to deformation and diseases. Therefore, the human spine should not carry more than 30 N•m moment for a long time, which will lead to deformation of the spine and the occurrence of diseases.

Validation of modal analysis of spinal thoracic segments T_7-T_{11} Validation

The first 6 orders of modal analysis were extracted from the T_7-T_{11} segment of the spine, and the results of modal analysis are shown in Table 4, and the description of the first 6 orders of revitalisation is shown in Table 5. The maximum amplitude and modal vibration pattern of the first 6 orders are shown in Fig. 7.

From Fig. 7, it can be seen that T_7-T_9 segment is the most serious deformation of the spine model, which is more likely to produce larger deformation than the other segments, and the vibration amplitude of T_7-T_9 segment is the largest, which indicates that this segment has a large accumulation of load, which produces a large amount of stress, and is more likely to lead to the scoliosis than the other segments. From the results of modal analysis, it can be seen that the intrinsic frequency range of T_7-T_{11} segment is concentrated in 6-35 Hz, so the human body environment should be far away from this frequency range, so as not to cause damage to the spine.

Table 4 The first 6 orders of intrinsic frequency of T_7-T_{11} section

Order	**T_7-T_{11} Segmental intrinsic frequency (Hz)**
1	6.1638
2	6.8304
3	24.8960
4	28.7350
5	33.0100
6	35.2960

Table 5 Description of the first 6 orders of vibration pattern of T_7-T_{11} section

Ordinal number	Description of Spinal Vibration Patterns
1	Swing around the x-axis to the left and right
2	Move back and forth around the z-axis
3	Twisting around the x-axis and bending to the left and right
4	Stretch up and down around z-axis
5	Slight rotation around the x and y axes
6	Swing back and forth around the y-axis

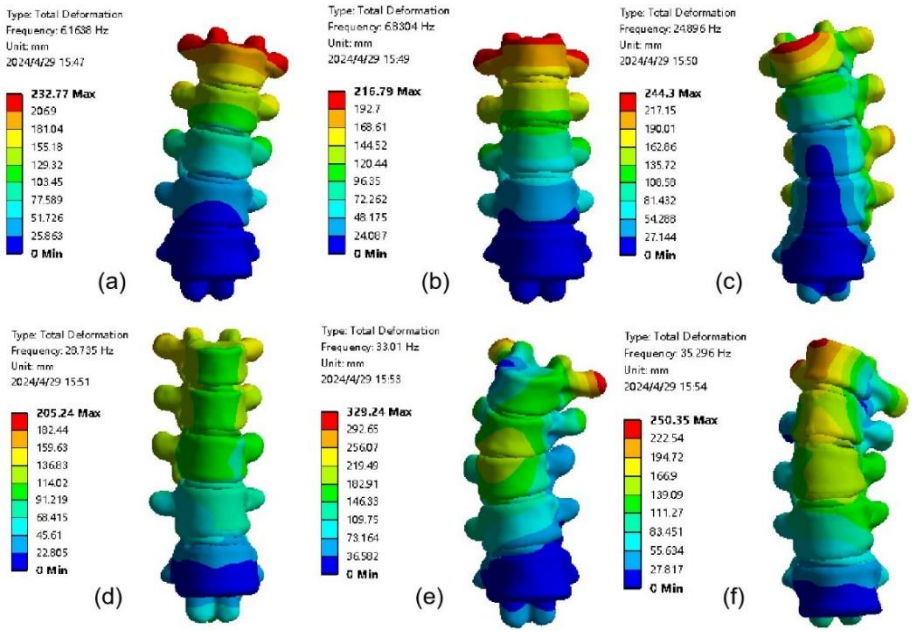

Fig. 7 Anterior 6th order vibration pattern of the spine

IV. CONCLUSION

The results of the static analysis show that the displacement value increases with the increase of the moment, and when the moment is less than 10 N•m, the displacement value of the thoracic spine segment stabilises within 3 mm, and even when the moment of 30 N•m is applied, the displacement value is less than the stabilised value of 3.5 mm, but it is in the critical state.And when the moment reaches 50 N•m, the displacement value of the thoracic spine segment is out of the stable range. The above conclusion shows that in order to keep the spine in a stable displacement range, the moment should be less than 30 N•m, so as to maintain the healthy state of the spine. If the moment exceeds 30 N•m, it will destroy the stability of the spine, which is not conducive to the healthy growth of the spine.

Through modal analysis, it can be seen that the amplitude of the T_7 segment of the thoracic spine is the largest in the vibration situation, and the closer to the T_7 segment, the larger the vibration amplitude is. By analysing the intrinsic frequency of the spine through modal analysis, people can be kept away from the environment similar to the intrinsic frequency; it has practical reference value to avoid resonance caused by the intrinsic frequency of the human body in engineering design.

In summary, through the finite element analysis of the spinal T_7-T_{11} segment, the measured mobility of the spinal T_7-T_{11} segment is similar to the results of the previous literature, which verifies the validity of the finite element model, and results in the stable range of the maximum displacement value of the spinal T_7-T_{11} segment and the range of the intrinsic frequency, the details of which are as follows

1. After finite element analysis, it is known that when the moment load is less than 30 N•m, the critical value of the spine displacement value is reached and the spine is in a stable state.
2. When the moment load reaches 50 N•m, the spine is in an unstable state, so the moment load should be kept within 30 N•m, so as to keep the spine in a safe range, which is conducive to the healthy growth of the spine.

3. By analysing the first 6 orders of modes of the spine, the modal intrinsic frequency of the spine is mainly concentrated in the range of 6-35 Hz, and the human body should be kept away from this frequency range in order to avoid damage to the spine.

REFRENCES

[1]. ZHANG YF,LI Shuai,LIU Ning,et al. Finite element modal analysis of the whole spine in adolescent idiopathic scoliosis[J]. Chinese Tissue Engineering Research,2024,28(30):4783-4787.

[2]. DU Juan, XIA Xiaoyu, MENG Lin, MIAO Jun, MING Dong. Progress in the application of spine biomechanics research based on coupled musculoskeletal dynamics and finite element model[J]. Journal of Applied Mechanics,2024,41(01):233-240.

[3]. HE Kai,XING Wenhua,LIU Shengxiang et al. Finite element method for modelling degenerative scoliosis: biomechanical analysis in etiology and treatment[J/OL]. Chinese Tissue Engineering Research,1-7[2024-03-09].

[4]. WON Yong-Jin,LI Xing-Lan,JING Sheng-Wei et al. Exploring the correlation between adverse spinal stress and fatigue syndrome based on finite element findings[J]. Clinical Journal of Traditional Chinese Medicine,2023,35(07):1273-127.

[5]. GAO Mingjie,DAI Lina,XU Yangyang et al. Finite element analysis of 14-year-old adolescents after spinal L4-5 segmental foraminoplasty based on TESSYS technology[J]. Journal of Anatomy,2023,54(03):335-341.

[6]. Hurwitz EL, Randhawa K, Yu H, Côté P, Haldeman S (2018) The Global Spine Care Initiative: a summary of the global burden of low back and neck pain studies. Eur Spine J 27(6):796–801.

[7]. Brittany S ,Mark D .Development and evaluation of sex-specific thoracolumbar spine finite element models to study spine biomechanics.[J].Medical biological engineering computing,2023.

[8]. Roth A K, Beheshtiha A S, van der Meer R, et al. Validation of a finite element model of the thoracolumbar spine to study instrumentation level variations in early onset scoliosis correction[J]. Journal of the mechanical behavior of biomedical materials, 2021, 117: 104360.

[9]. Li, X., hung N, Cheng Y H, Po H L, et al. Spinal phantom comparability study of Cobb angle measurement of scoliosis using digital radiographic imaging[J]. Journal of orthopaedic translation, 2018, 15: 81-90.

[10]. Zhu L, Wang J, Cao Y, et al. Finite element modeling construction of human lumbosacral vertebrae based on CT data[J]. Chinese Journal of Tissue Engineering Research, 2012, 16(30): 5511.

[11]. LI Rui,ZHANG Zhaojie,ZHANG Yanzhuo,et al. Effect of atlantoaxial joint disorder on biomechanical balance of upper cervical spine based on three-dimensional finite element analysis[J]. Chinese Orthopaedics and Traumatology,2024,32(03):59-64.

[12]. Guo L X, Lin T L, Li C L. Influence of joint injury on frequency characteristics of the spine[J]. Journal of Northeastern University (Natural Science), 2006, 27(6): 623.

[13]. Xu M, Yang J, Lieberman I H, et al. Lumbar spine finite element model for healthy subjects: development and validation[J]. Computer methods in biomechanics and biomedical engineering, 2017, 20(1).

[14]. Jia K. Design of personalised rehabilitation support for knee joint based on 3D printing technology [D]. Hebei University of Science and Technology 2022.

[15]. Luo Huiqing,Gülaiti Baiti Meizi,Parhati Reşti et al. Effects of different bone density trajectory internal fixation systems on lumbar L4-L5 segments[J]. Science Technology and Engineering,2021,21(16):6626-6631.

[16]. Dai Yunlei,Wei Ya,Wu Changbing et al. Finite element simulation of the effect of spinal endoscopic foraminoplasty on lumbar spine biomechanics[J]. Journal of Xi'an Jiaotong University (Medical Edition),2022,43(01):127-132.

[17]. Giwa, YANG Snapdragon,FU Rongchang,LI Pengju,et al. Finite element analysis of the influence of the trapezius muscle on the spine of severe Lenke type 1 scoliosis[J]. Medical Biomechanics,2023,38(06):1154-1159+1178.

[18]. GUO TU Sheng,JULETI BUYTI Meizi,TAO Jie et al. Effects of sand therapy temperature and blood perfusion on temperature and stress fields of knee joint[J]. Science Technology and Engineering,2021,21(08).

[19]. OU Bingjin,ZHOU Yunfan,CHENG Shunda,et al. Finite element analysis of thoracolumbar vertebral fracture fixed by adjustable spinal external fixator[J]. Journal of Clinical Orthopaedics,2023,26(06):885-889.

[20]. Jonas W ,Paolo F ,Marco S, et al.Kinematics of the Spine Under Healthy and Degenerative Conditions: A Systematic Review.[J].Annals of biomedical engineering，2019,47(7).

[21]. BODEN S D, WIESEL S A M W. Lumbosacral segmental motion in normal individuals have we been measuring instability properly[J]. Spine, 1990, 15(6): 571-576